Title

Non-catalytic glycerol dehydrogenation to dihydroxyacetone using needle-in-tube dielectric barrier discharge plasma.

Journal

Scientific Reports, 14(1)

Authors

Kongprawes, Grittima

Wongsawaeng, Doonyapong

Hosemann, Peter

et al.

Publication Date

2024-12-28

DOI

10.1038/s41598-024-82691-2

Peer reviewed

scientific reports

Check for updates

OPEN

Non-catalytic glycerol dehydrogenation to dihydroxyacetone using needle-in-tube dielectric barrier discharge plasma

Grittima Kongprawes[1], Doonyapong Wongsawaeng[1,7]✉, Peter Hosemann[2], Kanokwan Ngaosuwan[3], Worapon Kiatkittipong[4] & Suttichai Assabumrungrat[5,6]

Glycerol, a by-product of biodiesel production, could be converted into various value-added products. This work focuses on its dehydrogenation to dihydroxyacetone (DHA), which is mainly used in the cosmetics industry. While several methods have been employed for DHA production, some necessitate catalysts and involve harsh reaction conditions as well as long reaction times. A needle-in-tube type dielectric barrier discharge (DBD) plasma technique for catalyst-free and environmentally-friendly glycerol conversion into DHA via dehydrogenation process was investigated using 0.1 M glycerol dissolved in deionized (DI) water at ambient temperature and pressure. The optimal condition was 60 W input power, 5 mm gap distance between the end of the needle and the liquid surface, and 0.5 L/min He flow rate. The highest DHA yield of 29.3% was obtained at 3 h with a DHA selectivity of 51.6% and glycerol conversion of 56.9%. Although the system allowed over 80% of glycerol to transform after 5 h, the DHA yield decreased after 3 h because the DHA product could further react with the reactive species in the plasma. The catalyst-free DBD plasma technique offers a simple and environmentally conscious method for DHA production via the dehydrogenation of glycerol.

Glycerol ($C_3H_8O_3$) is a primary by-product of biodiesel production. For every 100 kg of biodiesel production, 10 kg of glycerol is generated (10 wt%). Global biodiesel production is projected to increase by 3% annually between 2021 and 2030 to reach about 50 billion liters. Therefore, crude glycerol capacity from the process is continuously growing to about 5 billion liters[1]. Crude glycerol derived from biodiesel production requires a purification process to remove impurities such as methanol, fatty acid methyl esters, residue catalyst, and soap to obtain purified glycerol with a glycerol content exceeding 95% [2]. Purified glycerol is widely utilized in the food, pharmaceutical, cosmetic, and energy industries[2,3]. However, the prices remain relatively low at about US $0.11 and US $0.66 per kg of crude and purified glycerol, respectively[4]. Therefore, various researchers have studied glycerol valorization via catalytic and biochemical conversion, such as oxidation, hydrogenolysis, dehydration, oligomerization, and so on[5]. The resulting products include glyceraldehyde, propanediol, acetol, alkane, syngas, etc. One challenging added-value product from glycerol is dihydroxyacetone or DHA ($C_3H_6O_3$).

DHA stands out as the most valuable derivative obtained from glycerol. It costs about 227 times higher than purified glycerol[6]. It has been primarily used as a self-tanning ingredient in cosmetic applications. The other applications are in the pharmaceutical, medical, and food industries[7,8]. Generally, DHA production

[1]Research Unit on Plasma Technology for High-Performance Materials Development, Department of Nuclear Engineering, Faculty of Engineering, Chulalongkorn University, Bangkok 10330, Thailand. [2]Department of Nuclear Engineering, Faculty of Engineering, University of California at Berkeley, Berkeley 94720, USA. [3]Division of Chemical Engineering, Faculty of Engineering, Rajamangala University of Technology Krungthep, Bangkok 10120, Thailand. [4]Department of Chemical Engineering, Faculty of Engineering and Industrial Technology, Silpakorn University, Nakhon Pathom 73000, Thailand. [5]Center of Excellence in Catalysis and Catalytic Reaction Engineering, Department of Chemical Engineering, Faculty of Engineering, Chulalongkorn University, Bangkok 10330, Thailand. [6]Bio-Circular-Green-economy Technology & Engineering Center (BCGeTEC), Department of Chemical Engineering, Faculty of Engineering, Chulalongkorn University, Bangkok 10330, Thailand. [7]Department of Nuclear Engineering, Faculty of Engineering, Chulalongkorn University, 254 Phayathai Road, Pathumwan, Bangkok 10330, Thailand. ✉email: Doonyapong.W@Chula.ac.th

can be achieved by the oxidation of glycerol via several processes: thermocatalysis[9,10], enzyme catalysis[11], electrocatalysis[12], and photocatalysis[13,14]. Among these techniques, thermocatalytic offers a high reaction rate and can be effectively employed for high concentrations of aqueous glycerol. Still, it often relies on catalysts derived from expensive noble metals: Pt, Pd, Au, and other alloys, as well as external heat (50–80 °C) and pressure (about 3 to 11 bar) for the reaction to proceed[4,15]. An enzyme catalyst provides high selectivity, but final product separation from the reaction mixture remains difficult[4]. Electrocatalysis and photocatalysis offer the advantage of converting glycerol under milder conditions. In the case of electrocatalysis, the reaction occurs by applying an electric potential to chemical cells, eliminating the need for noble catalysts. Therefore, the C-C bond scission is randomly generated[4]. The photocatalytic process has been improved using solar energy, a sustainable energy source. However, the process is often associated with prolonged reaction times and necessitates the use of a catalyst[4,14]. Combining photocatalytic and electrocatalytic methods offers less energy consumption of the system and avoids using costly noble catalysts. This technique has been developed and achieved a DHA selectivity of more than 70%, as reported in the investigation of Luo et al.[4]. The self-powered photocatalytic system energized by 2 V solar panels could be employed for DHA production from 0.1 M aqueous glycerol solution using Bi_2O_3/TiO_2 as a catalyst. The reaction took place at ambient conditions for 8 h, and the DHA selectivity reached 74.8%. Nevertheless, these mentioned methods proceed in the presence of a catalyst, which typically demands significant energy for catalyst preparation and regeneration. The photoelectrocatalytic method necessitates an electrolyte solution, so the pH of the solution is significant for the reaction performance. Bioconversion is also employed. The method presents a high yield of DHA production, but it requires bacteria preparation, pH control during the reaction, and a long reaction time, which could last up to 72 h, as indicated in the study of Ripoll et al.[16]. Normally, conversion of glycerol into DHA typically requires the dissolution of glycerol in a solvent serving as an oxidant. Common oxidant solvents include water, dimethyl sulfoxide (DMSO), and acetonitrile (CH_3CN), among others. The presence of these oxidant solvents helps reduce the viscosity of glycerol, thereby promoting a faster reaction rate[17].

To avoid harsh operating conditions (high pressure and temperature), the implementation of non-thermal plasma is a promising alternative technique for facilitating chemical reactions. Plasma is commonly regarded as the fourth state of matter. Artificial plasma can be generated by applying adequate energy, surpassing the ionization of substances, particularly gases. This process leads to the dissociation of gas molecules, forming a plasma state comprising energetic electrons, ions, excited, and neutral species, alongside the emission of light or photons[18]. In chemical reactions, plasma has been utilized to initiate and assist the chemical catalytic process. It is also applied to convert glycerol into gas and liquid products such as acrolein, propene, syngas, H_2, and others[19–21]. Plasma can improve the reaction performance and allow the reaction to proceed at milder conditions. For instance, the conventional gasification of glycerol typically necessitates temperatures ranging from 525 to 725 °C. However, by applying plasma, the temperature requirements can be substantially reduced to a range of 220 to 290 °C, eliminating the need for external heat sources[22]. Plasma has been successfully integrated with ultraviolet (UV) irradiation in the production of ammonia from natural water, obviating the need for a catalyst. This demonstrated the capability to generate substantial ammonia in regions exposed to plasma and UV[23,24]. Moreover, plasma has been practiced for the glycerol decomposition process to produce diverse valuable compounds without a catalyst[25–27].

Various types of plasma are employed in chemical reactions, including microwave, arc, dielectric barrier (DBD), radio frequency (RF), corona, and glow discharge plasmas. Each of these plasma techniques has its distinct generating conditions[28,29]. Among them, DBD is widely utilized due to its simple configuration, which consists of two electrodes separated by an insulating material. This setup allows for the propagation of plasma generated by an alternating current (AC) power supply throughout the electrode plates. DBD plasma can be generated at atmospheric pressure and at or above room temperature. Catalyst-free DBD plasma has found applications in liquid-phase reactions. For instance, it was employed in the cracking process of heavy oil to lighter composition[30]. Additionally, DBD plasma was utilized for the hydrogenation of edible oil without a catalyst, enabling the production of margarine with a similar texture to commercial margarine without trans-fatty acid formation due to the low operating temperature[31,32]. It was applied to produce hydrogenated biodiesel, resulting in enhanced oxidation stability[33,34].

Our previous work employed the DBD plasma reactor with a parallel-plate configuration for palm biodiesel hydrogenation using glycerol as a hydrogen donor[35]. The reaction took place at ambient temperature and pressure without a catalyst. The findings demonstrated that hydrogen atoms could be successfully extracted from glycerol molecules and bonded with the C = C bonds of biodiesel. Upon hydrogen extraction, the reacted glycerol, analyzed using a nuclear magnetic resonance spectrometer (NMR), exhibited peaks corresponding to glycerone, which were predicted to be dihydroxyacetone (DHA) and glyceric acid. This suggests that plasma technology could be employed for the dehydrogenation of glycerol to produce DHA under ambient conditions. In the present study, the needle-in-tube-type DBD plasma was utilized for glycerol conversion to DHA. To reduce viscosity, glycerol was dissolved in DI water. This plasma configuration generated a single strong plasma microfilament characterized by intense energetic electrons and reactive species. Moreover, unlike the parallel-plate-type plasma employed in our previous investigation[35], this configuration could well sustain the plasma in the presence of water, which could evaporate and generate moisture in the system. Notably, this represents the first and novel instance of applying the DBD plasma technique as an alternative method for the conversion of glycerol to high-value DHA. The system is simple and operates under ambient conditions without the need for a catalyst. This technique also offers the advantage of energy savings and environmental consciousness in catalyst processes, including preparation, separation, and regeneration.

Methodology

Experimental setup

The experimental setup employed a DBD plasma reactor, which consisted of a high-voltage (HV) stainless steel needle electrode (1 mm diameter and 160 mm length) inserted into a quartz tube (10 mm outer diameter, 1 mm wall thickness, and 110 cm length). A stainless steel plate (130 × 180 × 10 mm) was used as a ground electrode. The two electrodes were connected to a high-voltage, high-frequency power supply (neon sign transformer, Hongba brand, model HB-C10E), capable of delivering a maximum high voltage output of 10 kV and 30 mA with a fixed frequency of 25 kHz. A mixed solution of 60 mL glycerol and DI water was contained in a 400 mL borosilicate glass reaction chamber whose bottom acted as a dielectric material to separate the two HV electrodes and prevent arc. A magnetic stirrer was utilized throughout the reaction at 400 rpm. The input power to the system was regulated using a variac connected to the 220 V input section of the power supply, while a plug-in power meter recorded the consumed power during the reaction. He plasma gas was controlled and introduced into the reactor through a mass flow controller (Unit Instruments brand, model UFC-1260 A). A condenser was employed to condense the vapor produced by the reaction, and it also served as the gas outlet port. A thermometer was installed to observe the temperature change during the reaction. A high-voltage probe was connected to the needle electrode to measure the waveform of the high voltage via an oscilloscope (Tektronix brand, model TDS 2012). A drawing of the experimental setup is illustrated in Fig. 1.

Glycerol reaction by plasma

A specific solution concentration comprising glycerol (99.5% purity from KemAus) and DI water (produced locally in the laboratory), with a total volume of 60 mL, was admitted into the chamber. Air was purged out of the reaction chamber by continuously feeding He gas at a flow rate of 1 L/min for 1 min. During the reaction, the gas flow rate was adjusted to the desired value. As the bottom of the quartz tube was submerged in the solution, He gas provided through the tube resulted in bubbles in the solution. To generate plasma, the high-voltage, high-frequency power supply was energized. The stirring speed was set to 400 rpm to ensure effective solution mass transfer to react with the reactive species from plasma. The reaction was allowed for 1 h for reaction parameter optimization except in the investigation of reaction time. The parameters under investigation included input power (20–60 W), gas gap distance (1–10 mm), plasma gas flow rate (0.1–1 L/min), glycerol concentration (0.1–1 M), and reaction time (5–10 h). Herein, the impact of reaction temperature was excluded from the study based on previous research findings, which revealed that operating at ambient temperature provided the most suitable results and simplified the system[31,35]. Furthermore, operating at higher temperatures accelerated water evaporation, leading to increased viscosity of the reaction mixture. Each reaction parameter underwent duplication at least twice to ensure reproducibility.

Glycerol and product analysis

The feed glycerol and final products, including dihydroxyacetone (DHA) and possible by-products: hydrogen peroxide, ethanol, propanediol, and glycolic acid, were analyzed by gas chromatography-flame ionization detection (GC-FID). In the case of GC-FID analysis, the derivative was needed to obtain exact amounts of DHA in the solution because it is unstable at elevated temperatures. It can be converted into several derivatives, e.g., trimethylsilyl[36], diacetate[37], etc. Herein, it was transformed via acetylation by adding about 0.75 mL acetic acid and using 0.2 mL n-methylimidazole as a catalyst for a 15 mL sample. The reaction was allowed for 5 min at room temperature. To purify the sample, 1 mL of DI water was added and stirred; later, it was put in 1 mL

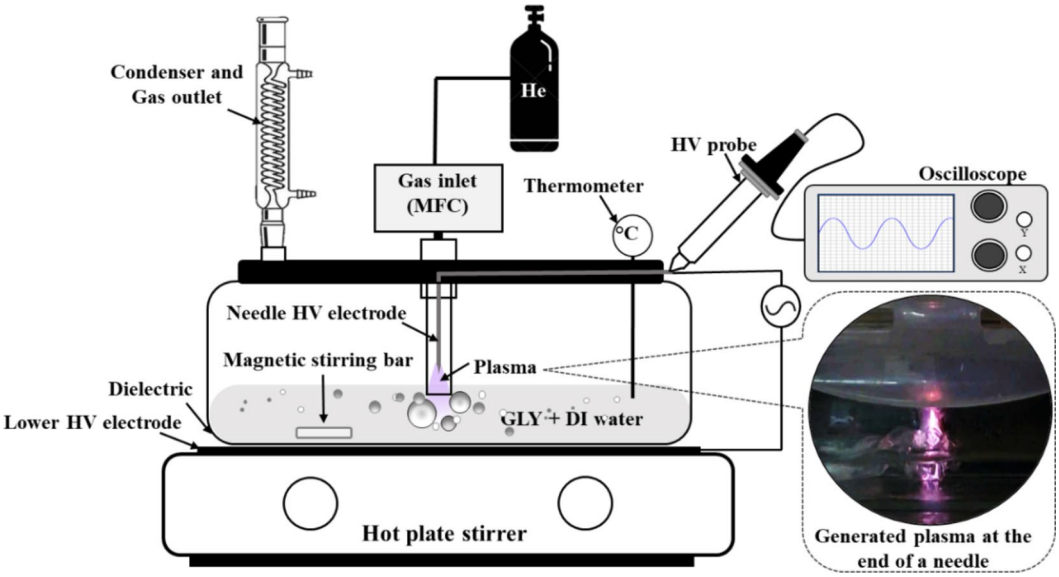

Fig. 1. Drawing of constructed needle-in-tube DBD plasma reactor.

dichloromethane and dried using anhydrous Na_2SO_4. Additionally, glycerol, DHA glyceraldehyde, formic acid, and lactic acid were inspected by high-performance liquid chromatography (HPLC). The GC-FID employed a Scion 8300GC instrument with a SCION-WAXMS GC column (30 m × 250 µm × 0.25 µm). The conditions were adapted from the study conducted by Egoburo et al.[38]. A split ratio of 50:1 was employed for the analysis, and He gas was utilized as the carrier gas with a constant flow mode at a rate of 2.5 mL/min. The oven temperature was maintained at 250 °C. The initial column temperature was set at 180 °C and held for 3 min. Subsequently, it was increased to 220 °C at a ramp rate of 40 °C/min and held for 2 min. A liquid sample volume of 1 µL was injected for composition analysis.

A stock solution of glycerol (GLY) and DHA (98% purity from Sigma-Aldrich) at 100 g/L was prepared by mixing GLY or DHA with DI water[39]. The stock solution was stored in a glass bottle in a refrigerator at 4 °C. To establish a calibration curve, serial dilutions of GLY or DHA in DI water, ranging from 0.1 to 50 g/L, were measured, and the area response was recorded.

The percentage of GLY conversion, DHA yield, and selectivity were calculated using Eqs. (1), (2), and (3), respectively. The selectivity of DHA could be calculated by the proportion of the amount of DHA to reacted glycerol instead of to total generated products, as present in the study of Imbault et al.[13].

$$\%\ \text{Conversion},\ (\text{X})_{\text{GLY}} = \frac{\text{Mole of GLY reacted}}{\text{Mole of GLY fed}} \times 100\% \tag{1}$$

$$\%\ \text{Yield},\ (\text{Y})_{\text{DHA}} = \frac{\text{Mole of DHA}}{\text{Mole of GLY fed}} \times 100\% \tag{2}$$

$$\%\ \text{Selectivity},\ (\text{S})_{\text{DHA}} = \frac{\text{Mole of DHA}}{\text{Mole of GLY reacted}} \times 100 \tag{3}$$

The high-performance liquid chromatography (HPLC, Varian ProStar) was equipped with UV visible detectors at wave numbers of 210 nm. The HPLC condition was modified from the study of S. Liebminger[40]. The sample was filtered, and then about 20 uL was injected into the column of Rezex ROA-Organic Acid Aminex HPX-87 H (300×7.8 mm). The column temperature was set at 60 °C. The solution of 0.5 mM of H_2SO_4 was used as the mobile phase with a flow rate of 0.6 mL/min. The run time was set at 30 min. This technique was used to analyze the other products that were not able to be detected by GC-FID. The products included glyceraldehyde (GLD), glycolic acid (GLYCOA), and formic acid (FA).

Results and discussion

Effect of input power

The input power was investigated at 20, 40, and 60 W. The lowest power to allow plasma to occur was about 20 W, while the high-voltage, high-frequency power supply coupled to the constructed plasma chamber consumed a maximum power of about 60 W (variac setting at about 220 V). Other parameters remained fixed at 5 mm gap distance, 0.5 L/min He flow rate, and 0.1 M glycerol concentration. The reaction took place for 1 h. During the reaction, plasma self-heating caused the temperature of the solution to rise to approximately 40, 50, and 60 °C for applying 20, 40, and 60 W, respectively. Since DHA is a high-value product from glycerol dehydrogenation, it is the preferred product. Therefore, the DHA concentration formed in the reaction was used to find the optimal parameter of the reaction. The findings were presented in Fig. 2, which demonstrated that higher input power led to increased DHA and reduction of GLY. To determine the power delivered to the electrode to generate plasma, a high-voltage probe and current monitor were connected to the system. It was found that the elevated power input also resulted in a higher discharge voltage at the electrode as well as current: peak-to-peak voltage of 1.5, 1.0, and 0.6 kV_{p-p} and current (I_{rms}) of 24.4, 15.3, and 6.9 mA at 60, 40, and 20 W, respectively. The discharge

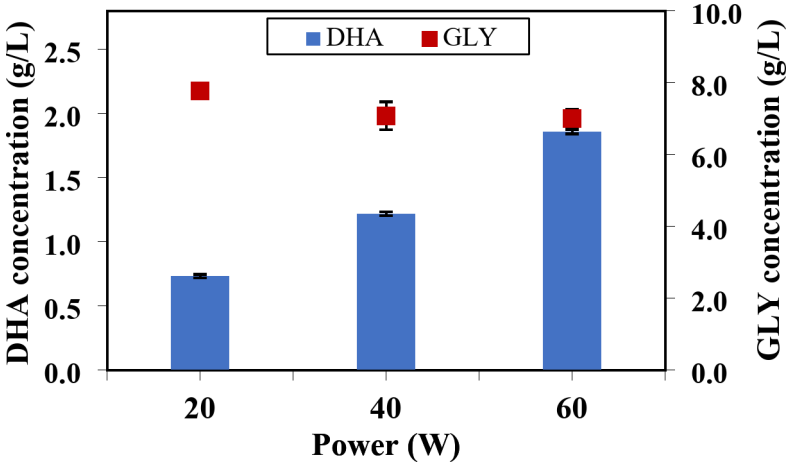

Fig. 2. Effect of input power on DHA production (5 mm gap distance, 0.5 L/min He, 0.1 M GLY concentration, and 1 h).

voltage was calculated to determine the discharge power by converting V_{p-p} to V_{rms}. In each input power case, V_{rms} was orderly presented at 0.53, 0.35, and 0.21 kV. The plasma discharge power is a function of frequency as presented in Eq. (4) [41].

$$P_{\text{plasma}} = f \int_{t_1}^{t_2} V(t) \cdot I(t)\, dt \tag{4}$$

where f is the pulse repetition rate, and V(t) and I(t) are the voltage and current of the product during the plasma time pulse duration, which is the energy consumed during one discharge period.

However, the frequency of each input power shown in the oscilloscope was not different, about 22.8 kHz. This is because the power supply utilized in this study was a fixed-frequency type. Based on the same contact time the actual plasma generation power was estimated from V_{rms} and I_{rms}, and the obtained plasma discharge power was only 12.9, 5.4, and 1.5 W for 60, 40, and 20 W of input power, respectively. Therefore, the efficiency of the power supply estimated by input power and obtained discharge power was approximately 14%. This is because 86% was lost as heat due to a significant impedance mismatch between the power supply and the DBD plasma chamber. Substantial DHA production of 1.9 g/L was achieved at the supplied power of 60 W with a DHA yield of 19.0% and a GLY conversion of 29.9%. The GLY conversion using 40 and 60 W was similar, but DHA was produced more at 60 W. This is because 60 W provided about 10 °C higher than 40 W, promoting dehydrogenation, which is the endothermic reaction of glycerol. Additionally, the higher supplied power caused higher temperatures, so it increased water evaporation to be in the gas phase. Both evaporated water and power affect the plasma morphology, causing it to contain a hotter and higher number of plasma filaments[42]. In the present study, a larger plasma filament was observed to form around the end of the needle electrode, and the plasma light was also brighter and more diffused when high plasma power was supplied, as presented in Fig. S1. This led to higher water molecules in the gas phase and at the gas-liquid interface to be dissociated, becoming radicals, including $H^{\bullet}$, $O^{\bullet}$, and $OH^{\bullet}$ radicals, as well as H_2O_2[42]. It was reported that $OH^{\bullet}$ has the potential to dominate glycerol decomposition[43]. Thus, this induced the dehydrogenation of glycerol reaction, facilitating the formation of DHA.

Effect of gap distance

The impact of different gap distances was studied at 1, 5, and 10 mm, for the minimum distance to prevent the end of the HV needle electrode from contacting the solution was approximately 1 mm. The largest gap distance of 10 mm could sustain the plasma at 60 W. The reaction was conducted at 60 W, 0.5 L/min He flow rate, and 0.1 M glycerol concentration for 1 h. As demonstrated in Fig. 3, the result shows a significant difference in DHA production based on the gap size. The 5 mm gap yielded higher DHA production (1.9 g/L) than at 1 and 10 mm, which generated DHA of 1.7 and 1.6 g/L, respectively. This is because the gap between the two electrodes directly influences the formation of energetic electrons and reactive species in the plasma state[19]. A narrower gap requires lower energy input into the system, resulting in a lower plasma density than a larger gap[44,45]. On the other hand, a larger gap resulted in a longer traveling distance for the reactive species, increasing the probability of recombination between electrons and positive ions before they reached and collided with the glycerol molecules. Additionally, energetic electrons may lose their kinetic energy through collisions with other electrons and species, affecting the DHA production to decrease. In conclusion, the most suitable gap size for optimal DHA production of 1.9 g/L in the designed plasma reactor was 5 mm.

Effect of he gas flow rate

The plasma carrier gas flow rate was varied and it was found that the minimum value that could generate plasma at 60 W without burning at the end of the HV needle electrode was about 0.1 L/min. Therefore, the gas flow rate of 0.1, 0.5, and 1 L/min was examined under fixed conditions of 60 W, 5 mm gap distance, and 0.1 M glycerol concentration for 1 h. Figure 4 indicates that the optimal condition for DHA production of 1.9 g/L was achieved at the flow rate of 0.5 L/min, followed by flow rates of 1 and 0.1 L/min, which resulted in the same amount of DHA production of 0.3 g/L. The carrier gas flow rate plays a significant role in plasma reactions because it affects filament breakdown and the charge transfer equilibrium. The study of Hoft et al.[46] found that the convection and balance of charged particles and excited species in the plasma were influenced by the plasma gas flow rate.

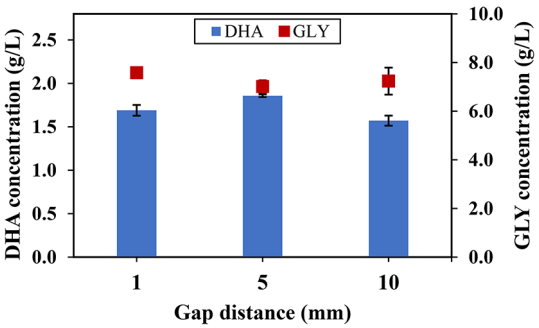

Fig. 3. Effect of gas gap distance on DHA production (60 W, 0.5 L/min He, 0.1 M GLY concentration, and 1 h).

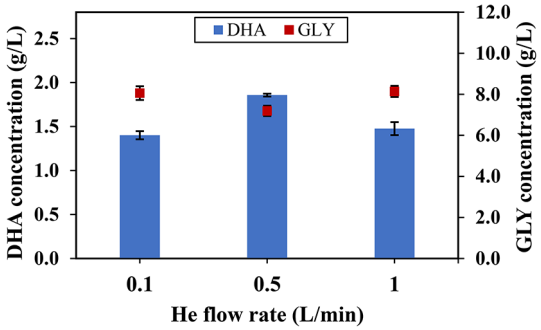

Fig. 4. Effect of He gas flow rate on DHA production (60 W, 5 mm gap distance, 0.1 M GLY concentration, and 1 h).

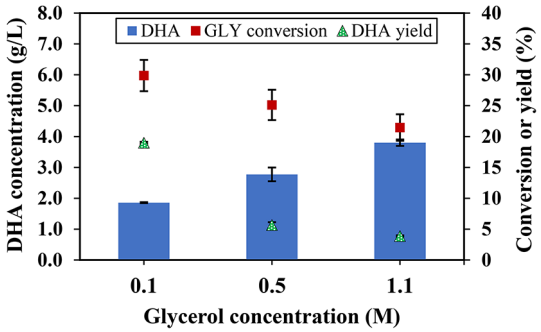

Fig. 5. Effect of GLY concentration on DHA production, yield, and GLY conversion (60 W, 5 mm gap distance, 0.5 L/min He, and 1 h).

A higher gas velocity induced a larger diameter of filaments, which compost generated reactive species in the system. The residence time of the gas in the system was inversely proportional to the flow rate. It was reported that the diameter of the filament was greater when the residence time was shorter, corresponding to the high gas flow rate[46]. In this present work, the residence time of the gas in the reactor was 3.40, 0.68, and 0.34 min for 0.1, 0.5, and 1.0 L/min, respectively. In addition, the peak-to-peak voltage of the different supplied gas flow rates was determined. The findings shown in Fig. S2 were at the constant applied plasma power of 60 W, with the peak-to-peak discharge voltage of 1.0, 1.5, and 1.84 kV for 0.1, 0.5, and 1.0 L/min gas flow rate, respectively. The result is consistent with the findings in the study of Qiang[47]. They found that the power increased when the speed of gas flow was high when the plasma current was fixed. Hence, the voltage relatively rose as power is a function of voltage and current for the DC power supply system utilized in their work. In our study, a higher gas flow rate offered a higher discharge voltage. Therefore, the gas was more possibly dissociated/ionized as the voltage trended to exceed the required gas breakdown voltage, influencing the generation of a large plasma filament. However, the high gas flow rate (1.0 L/min) limited the time for the reaction to occur as it provided a short contact time and possibly carried the reactive species that should have collided with the solution out of the reactor. In comparison, the lowest flow rate (0.1 L/min) offered longer residence time but less discharge voltage to excite He gas. Consequently, it can be concluded that the flow rate of 0.5 L/min was the most favorable condition for DHA production in the designed plasma reactor.

Effect of glycerol concentration

The glycerol concentration was experimented with at 0.1 M because this was a concentration investigated by other studies that used water as a solvent for glycerol conversion to DHA. Then, the glycerol concentration was increased to 0.5 and 1.1 M, the maximum concentration applied in catalytic reaction[10] to discover the maximum production capacity. The reaction was conducted at 60 W, 5 mm gap distance, and 0.5 L/min He for 1 h. The result is illustrated in Fig. 5. More DHA was generated with higher glycerol concentration. There was a significant difference in DHA production of 1.9, 2.8, and 3.8 g/L for 0.1, 0.5, and 1.1 M glycerol concentrations. On the contrary, the conversion or yield reduced with increasing glycerol concentration. 0.1 M offered the highest yield of 19.0%, followed by 0.5 and 1.1 M providing 5.7 and 3.9% yield, respectively. It should be noted that the DHA productivity rate did not increase proportionally with the glycerol concentration because the kinetics of the reaction depend on many factors, such as reaction order, viscosity of the reaction mixture, and plasma power. In this study, the plasma power was at 60 W while varying the glycerol concentration. Additionally, the reactions could be hindered by other limitations, such as mass transfer, where higher glycerol feed content increases viscosity, thereby delaying electron transfer[48] within the solution, as well as the ions/electrons mobility, which

is inversely proportional to the liquid viscosity as described by Stokes' law[49] in Eq. (5) when the movement of charged particles is defined as a sphere in the liquid.

$$\mu_{ion} = \frac{e_0}{6\pi\,\eta\,R_{ion}} \tag{5}$$

Where μ_{ion} denotes ion mobility; e_0 is the electronic charge; η and R_{ion} stand for liquid viscosity and the ion fictitious radius, respectively.

The yield of DHA was not equal to the conversion of glycerol. This is because some of the reacted glycerol molecules may undergo further interactions with reactive species, leading to the formation of other glycerol derivative products instead of DHA. Therefore, 0.1 M was the most reasonable concentration, offering most glycerol molecules successfully converting to DHA.

Effect of reaction time

The optimal condition obtained earlier (60 W, 5 mm gap distance, 0.5 L/min He, and 0.1 M GLY concentration) was employed for the reaction time investigation up to 5 h. As depicted in Fig. 6 (a), the results revealed that glycerol was continuously converted. At the same time, DHA increased with time from the beginning to 3 h with the DHA production of 2.9 g/L, DHA yield of 29.3%, and glycerol conversion of 56.9%. While glycerol conversion continued to rise and reached 82.8% at 5 h, DHA production exhibited a decreasing trend, with concentrations of 2.5 g/L (25.9% DHA yield) and 2.7 g/L (28.10% DHA yield) observed at 4 and 5 h, respectively. This decline in DHA production might be because the reactive species in the system started to react with DHA rather than glycerol as the glycerol content in the reactor decreased over time. Hence, the generated DHA was transformed into other products. In the study of Walgod et al.[10], the conversion of aqueous glycerol to DHA was conducted via catalytic oxidation under high-pressure conditions for up to 8 h. The investigation used a Pt5%-Bi1.5%/AC catalyst, and a glycerol conversion of 84% with a DHA yield of 36% was achieved at 2 h. However, at 5 h, the yield decreased to approximately 25% at a conversion of nearly 100%. The finding in this referencing work is similar to the present investigation in that the DHA would be less produced when the reaction time was longer, causing the DHA yield and selectivity to decrease.

Figure 6 (b) presents the DHA and glyceraldehyde (GLD) production over 5 h of the reaction time at the most suitable condition of 0.1 M GLY concentration. The result shows that GLD was generated less than DHA at every point. This is because the energy required in the reaction to produce DHA was lower than that of GLD, as explained in Sect. 3.8, plasma reaction mechanism. Additionally, it was reported that DHA has high thermodynamic stability compared to GLD[7]. DHA is more inert and difficult to transform into other small products. At 3 h of the reaction time, about 1.89 g/L of GLD was produced with a yield of 19.28%. Then, at 5 h, it decreased to 1.46 g/L with a yield of 15%. This is because GLD could be easily activated by the reactive species in the plasma to become other products, resulting in its lesser content in the mixed solution.

A concentration of 0.5 M was additionally investigated for up to 10 h to observe the behavior of DHA production at higher glycerol concentrations. As demonstrated in Fig. 6 (c), the results present that at 5 h of reaction time, the glycerol conversion and DHA yield were 47.2 and 22.7%, respectively. For 10 h, the glycerol conversion reached 63.5%, with a DHA yield of 28.1%. The DHA was continuously produced until 10 h because the system contained a substantial amount of unreacted glycerol. However, it was observed that the selectivity turned to reduce from 48.0 to 44.2% at 10 h. This is consistent with the reaction behavior noticed in the 0.1 M glycerol concentration; DHA could be activated and transformed into other products by plasma.

For 0.1 M, the most suitable reaction time to acquire the highest yield of DHA was 3 h, providing the glycerol conversion of 56.9%, DHA yield of 29.4%, and selectivity of 51.6%. Comparatively, at a higher concentration of 0.5 M, the DHA yield and selectivity were lower, even after a longer reaction time of 10 h. The DHA yield and selectivity of the 0.5 M case were 28.1 and 44.2%, respectively, at a glycerol conversion of 63.5%. The productivity rate for the case of 0.1 and 0.5 M were 0.96 and 1.37 g/L•h, respectively. However, the plasma process has limitations of low selectivity and uncontrollability. Considering that similar products generated by glycerol dehydrogenation initially become DHA or GLD, the repeatability in this study showed that DHA production was significantly higher than GLD production in the case of 0.1 M. The reaction needs to be conducted for at most 3 h under the most suitable condition to obtain mainly DHA with more than 50% selectivity.

In comparison to other studies, various methods for producing DHA from glycerol, such as photocatalytic, electrocatalytic, photo combined with electrocatalytic, catalytic oxidation, and bioconversion, have been studied, as demonstrated in Table 1. In terms of productivity rate under optimal conditions for each process, the plasma technique employed in the present investigation outperforms photocatalytic approaches that utilize the TiO_2 catalyst, as well as electrolytic, photoelectrolytic, and bioconversion methods. However, it is important to note that the initial glycerol concentration influences productivity. With higher initial glycerol concentrations, DHA can be produced at a faster rate.

Since DHA is the desired product, its selectivity should be considered. High selectivity displays a high DHA yield and facilitates its separation from other by-products. Using a catalyst in oxidation reactions under high pressure offers advantages such as fast reaction rates and increased selectivity. The method can be employed for high glycerol concentrations compared to other methods, resulting in a higher productivity rate. The plasma technique is inferior to the photocatalytic using flowers-like Bi_2WO_6 catalyst, electrocatalytic, and photoelectrocatalytic processes. These methods rely on catalyst modifications to enhance glycerol absorption, enabling specific reactions at the secondary hydroxyl group for efficient DHA production[10,14,50]. In conclusion, the utilization of the plasma technique demonstrated a higher productivity rate and DHA selectivity compared to the photocatalytic method employing a TiO_2 catalyst, although DHA selectivity was lower compared to several other techniques listed in Table 1.

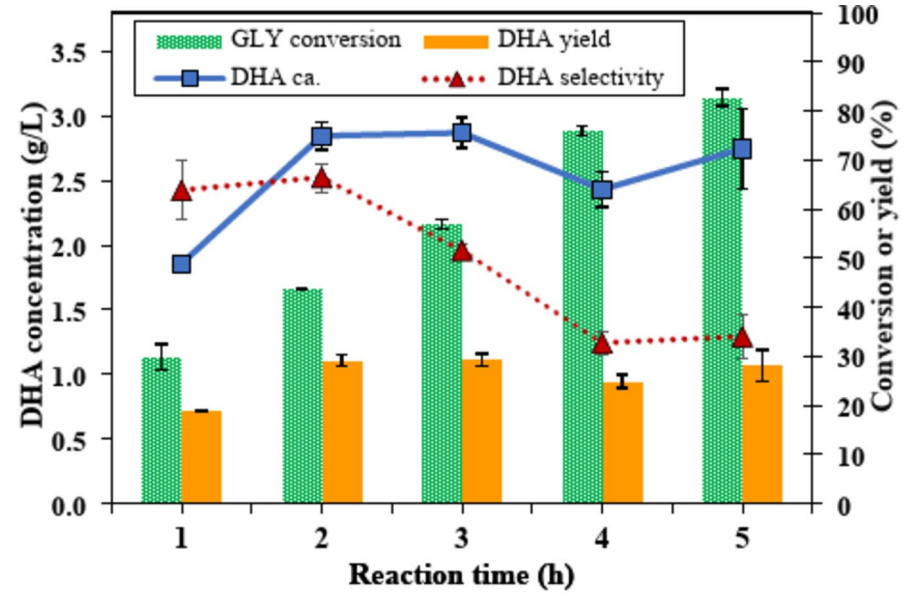

(a)

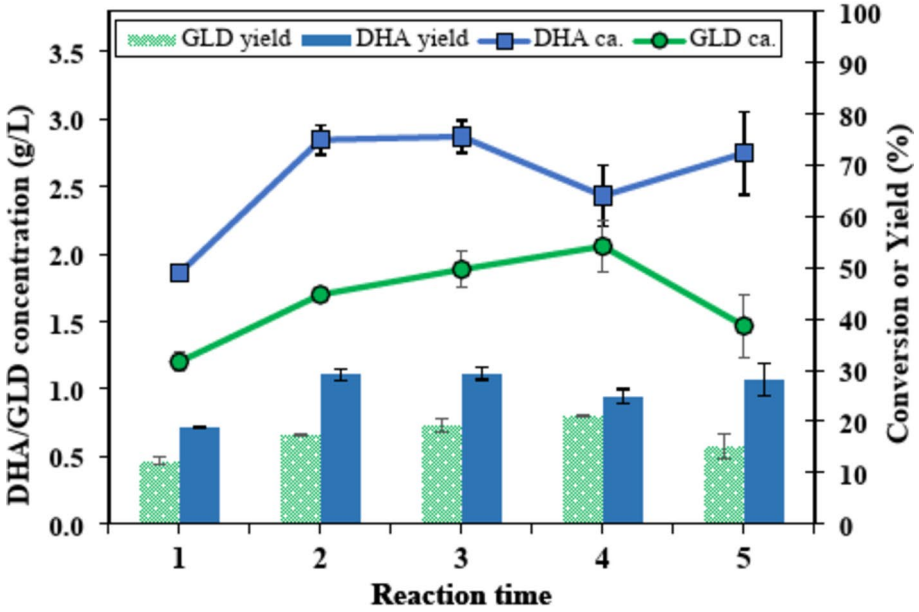

(b)

Fig. 6. Effect of reaction time on DHA production, yield, and GLY conversion for (**a**) 0.1 M GLY concentration, (**b**) DHA and GLD production at 0.1 M GLY concentration and (**c**) Effect of reaction time for 0.5 M GLY concentration (60 W, 5 mm gap distance, and 0.5 L/min He).

While the product yield in this study is relatively low when using plasma in isolation, the results highlight the inherent potential of plasma technology as a powerful technique for chemical transformation. With further optimization, plasma can be significantly enhanced by coupling it with complementary techniques, such as plasma-assisted catalysis, or by integrating methods like ultrasound-assisted or microwave-assisted plasma, paving the way for more efficient and versatile applications. For its application, the current findings from the

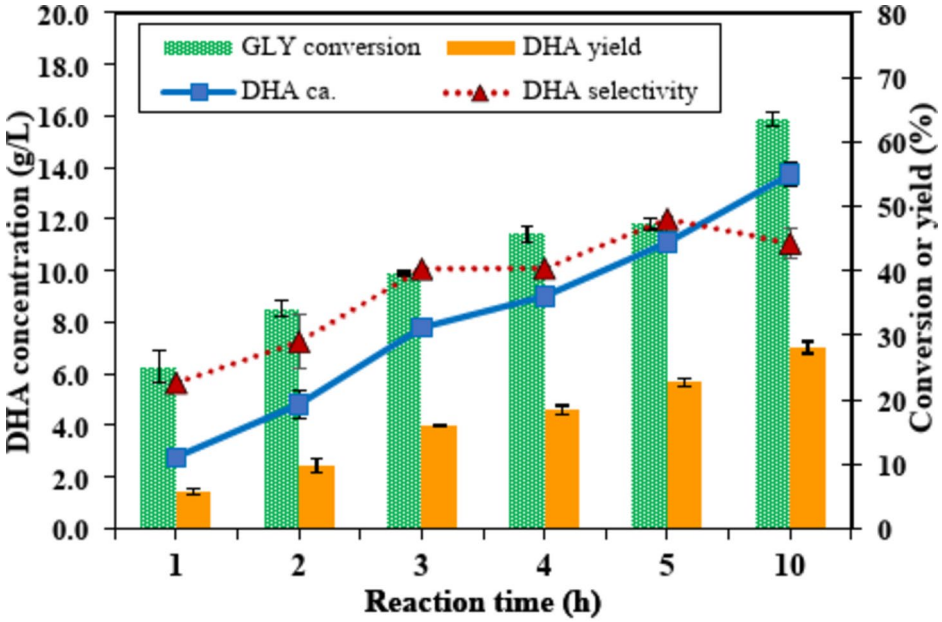

(c)

Figure 6. (continued)

Method	Initial GLY ca. (M) in solvent	Optimal condition	Y_{DHA}, S_{DHA} (%)	X_{GLY} (%)	Productivity rate (g/L h)	Refs.
Photocatalysis	4×10^3 in water or acetonitrile	1 g/L TiO_2 loading at ambient condition[a] for 5 h	Water: Y = 5.3, S = 14.7 Acetonitrile: Y = 17.2, S = 17.8	Water: 36.1 Acetonitrile: 96.8	Water: 3.8×10^{-3} Acetonitrile: 12.4×10^{-3}	13
Photocatalysis	N/A in water	Bi_2WO_6 catalyst at ambient condition[a] for 5 h	Y = 87 S = 91	96	–	14
Catalytic oxidation	1 in water	10 wt% Pt5%–Bi1.5%/AC loading at 80 °C, 3.5 bar for 2 h	Y = 36 S ≈ 42.8	84	13.6	10
Electrocatalysis	0.1 in water	Glycerol solution mixed with 0.5 M H_2SO_4 using PtSb/C catalyst, anode potential = 0.797 V at 60 °C for 10 h	Y = 61.4 S ≈ 68	90.3	0.6	12
Photoelectrocatalytic oxidation	0.1 in water	Bi_2O_3/TiO_2 photoanode, self-powered PEC system equipped with solar panel = 2 V, illumination area = 7 cm^2, 0.5 M Na_2SO_4 electrolyte, solution pH = 2 for 5 h	Y = N/A S = 74.8	> 50%	7.8×10^{-3}	4
Bioconversion	0.5 crude glycerol in water	Agar immobilized Gox catalyst at 30 °C in shake flask with 180 rpm agitation rate for 72 h	Y = 87 S = N/A	–	0.6	16
Plasma dehydrogenation	0.1 in water	60 W, 5 mm gap distance, and 0.5 L/min He for 3 h	Y = 29.4 S = 51.6	56.9	1.0	This work

Table 1. Performance comparison for DHA production from glycerol using various methods. [a]Ambient condition = ambient temperature and pressure.

plasma technique in this study could serve as a foundation for producing other products by improving some parts of the system. For instance, a stirring mechanism should facilitate better mass transfer, and the reactor should include several more high-voltage electrodes. This way, plasma can be generated across almost the entire surface of the liquid and interact more effectively with the aqueous glycerol. The technique can be the basis for scaling up plasma applications. However, there is not much research on liquid raw materials for large-scale plasma systems. It is mainly used for gas decomposition, e.g., benzene[51], air[52,53], and so on. The plasma for liquid treatment, like glycerol conversion into DHA, can be considered for large-scale production by conducting in a hybrid system, which is a combination of plasma and other processes as recommended in the study of Okubo[52]. This will provide an advantage in power consumption reduction. While it is true that plasma-based processes have not yet become mainstream in large-scale industrial applications, several pilot-scale projects and/or industry collaborations are actively exploring its potential for selective conversion in areas such as dried

herbs treatment[54], bioactive compounds of tomato preservation[55], odors and chemical pollutants removal[56,57], and bondability of wood improvement[58]. Furthermore, as industries move toward more sustainable and energy-efficient processes, plasma technology may become a viable alternative in certain niche applications.

The plasma had the potential to convert glycerol to DHA, but other by-products were also generated during the reaction due to the random reaction characteristic of plasma. This inherent plasma characteristic also affects the selectivity of DHA when different glycerol sources are utilized in the reaction. Using high-purity vs. crude glycerol to convert into DHA could offer dissimilar results. This is because crude glycerol contains impurities such as residue short-chain alcohol, catalyst, water, ash, and matter organic non-glycerol (MONG)[59] that could be dissociated by plasma reactive species and incorporated with the glycerol molecule, resulting in other products generated instead of DHA. This is a challenge and should be investigated in future work.

In comparison with aqueous glycerol treatment by plasma, Bang et al.[43] studied plasma-induced glycerol transformation to produce formic acid. It was found that a proportion of water in aqueous glycerol assisted in generating more formic acid and other products, including hydroxyacetone, glyceraldehyde, and dihydroxyacetone. This is because the water contained in glycerol resulted in the production of $OH^{\bullet}$ radicals, which continued the further reaction. At a specific input energy (SIE) of 384 kJ/L, glycerol volume fraction of 0.1, total liquid volume in a reactor of 30 mL, Ar plasma gas flow rate of 0.2 L/min, and applied peak voltage of 16 kV, the formic acid was formed at 674 ppm. The exact amount of DHA and other products was not indicated in this study.

When SIE was defined as the plasma processing time (t_p) multiplied by the power density, which was the ratio of discharge power (P_d) to the volume of aqueous glycerol (Q)[43], the present investigation, under the most suitable condition of 60 W, 60 mL, and 3 h, results in the SIE of only 0.33 kJ/L. The energy supplied to the system was much lower than that in the previous study, so the products were still mainly DHA and GLD. This implies that the previous study applied sufficient energy to break the glycerol molecules into a small molecule like formic acid. At the most suitable condition presented in Table 1, DHA was formed at 2.8 g/L. Therefore, the energy required to produce one gram of DHA in the designed system was 0.12 kJ. When applying the plasma power of 60 W for 3 h, the power needed to generate 1 g of DHA was 0.35 W.

FTIR analysis

To be analyzed by FTIR, feed glycerol and reacted solution of 0.1 M glycerol after plasma reaction at 60 W, 5 mm gap distance, and 0.5 L/min He for 3 h were oven heated at 110 °C for 8 h to facilitate the evaporation of water from the glycerol/DHA and other high-boiling point products. After evaporation, the feed glycerol exhibited a clear color, whereas the reacted glycerol showed a noticeable brown hue as presented in Fig. 7 (a). This color change was primarily influenced by the presence of DHA in the mixed solution, particularly when exposed to high temperatures[60]. Figure 7 (b) illustrates the obtained FTIR spectra. Pure glycerol refers to freshly sourced glycerol directly from the bottle, while feed glycerol denotes the glycerol solution obtained after evaporation. Both pure and feed glycerol exhibited the same functional groups. The O-H stretching vibration was observed at a wave number of 3290 cm^{-1}, while the peaks at 2880 and 2930 cm^{-1} corresponded to symmetric and asymmetric stretching of C-H bonds. The C-OH in-plane bending appeared at 1413 and 1455 cm^{-1}. The peaks at 1212 and 1332 cm^{-1} represented CH_2 wagging. The stretching of the C-O bond is assigned to wave numbers 990, 1112, and 1034 cm^{-1}, with the final peak at 924 cm^{-1} attributed to the stretching of C-OH bonds[61,62].

For the case of the reacted glycerol, all of the characteristic peaks observed earlier in pure and feed glycerol were also detected. However, it was observed that the intensities of the O-H peak at 3290 cm^{-1} in Fig. 7 (c), as well as those of the peaks corresponding to C-O at 1112 and 900 cm^{-1}, were lower compared to feed glycerol. Interestingly, a new peak appeared at 1735 cm^{-1}, indicating the presence of C=O stretching and implying that the reactive species successfully broke the hydrogen atom bonding with oxygen (-COH) in glycerol, forming a ketone group (C=O). Moreover, it can be inferred that glycerol molecules did not bond with each other to form di- or triglycerol. This conclusion is supported by the fact that the peak at 1112 cm^{-1}, which is also associated with C-O-C stretching, did not become stronger but turned fairly weakened after the transformation of C-O bonds[61]. This suggests that the reactive process primarily involved the modification of individual glycerol molecules rather than polymerization into larger structures.

By-products analysis

The by-products besides DHA were inspected by GC. It was observed that glycerol exhibited a high sensitivity when using the SCION-WAXMS column. In Fig. S3 (a), at a concentration of 3 g/L for both glycerol and DHA, it was observed that the peak corresponding to glycerol had a significantly larger area, approximately 94.8% of the total peak area. In contrast, the peak area attributed to DHA was only 3.8%, and the remaining 1.3% was water. Fig. S3 (b) illustrates a comparison between the peak of feed glycerol (0.1 M) and the reacted glycerol or product obtained from the plasma reaction under the conditions of 60 W power, a 5 mm gap distance, and a helium flow rate of 0.5 L/min for 5 h. The green line corresponds to the feed glycerol, with the peaks at 1.18 and 4.74 min representing water and glycerol, respectively. The pink line represents the product, showing a detected peak of DHA at a retention time of 3.73 min with several peaks near the peak of water. The peaks at 1.18, 1.36, 1.43, 1.53, and 1.67 min correspond to those observed by injecting 35% H_2O_2 into the GC-FID system, but they were lower intensity than those appearing in the product, as shown in Figs. S3 (c) – (d). This H_2O_2 was formed by plasma activation of water, as evidenced by the weakening of the water peak in the product.

To analyze other possible products in this reaction, the GC condition was held for 15 min instead of 6 min. The findings revealed no significant peak after glycerol. Moreover, the standard ethanol and propanediol, the possible by-products in this reaction, were analyzed in the same condition. Their peaks appeared at 1.17 and 2.06 and were not present in the product peaks.

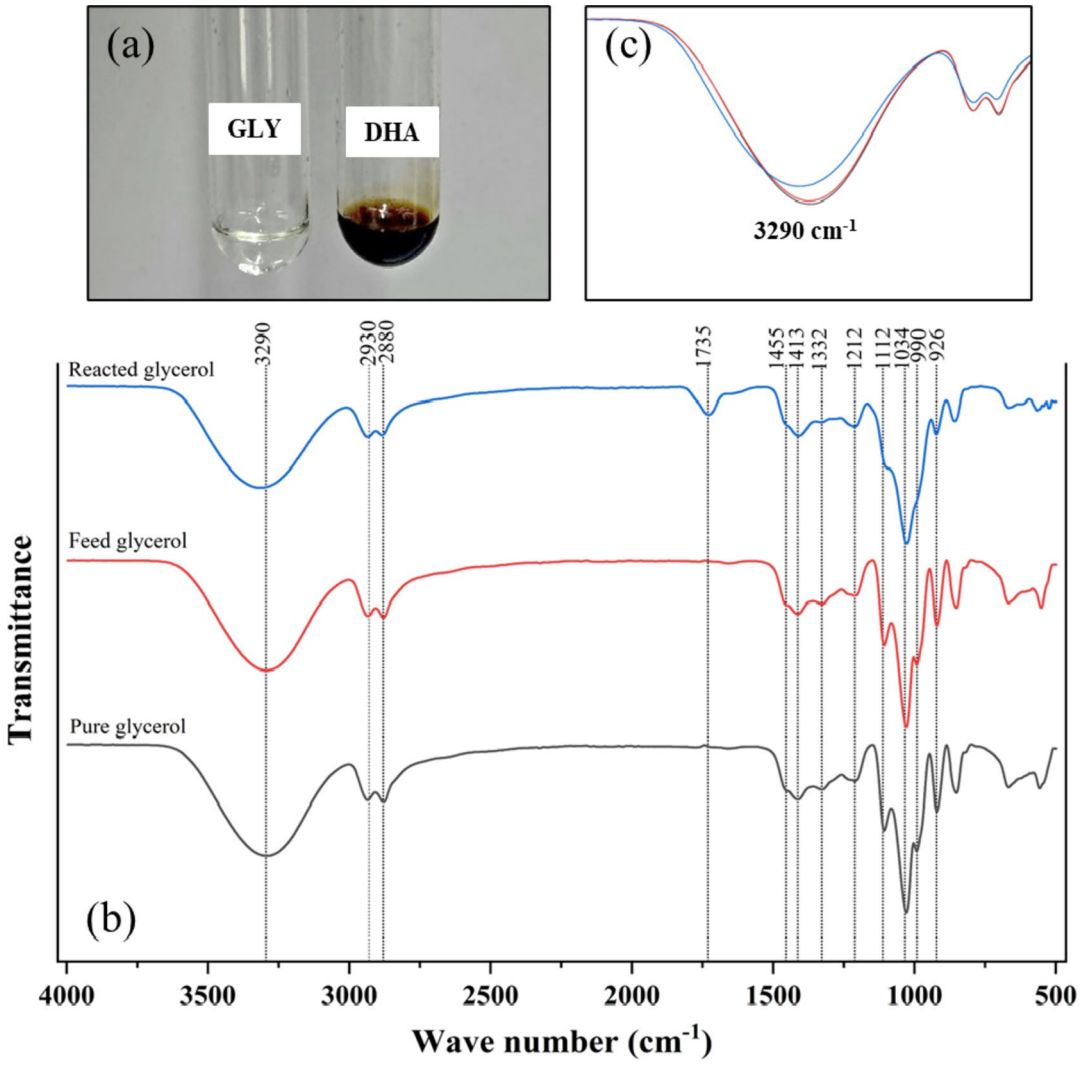

Fig. 7. (**a**) Evaporated feed glycerol and DHA product, (**b**) FTIR spectra of pure, feed, and reacted glycerol, and (**c**) –OH peak obtained from FTIR.

Moreover, the observed pH of the product decreased from about 6.0 to 3.8 after 5 h of reaction time. This might be due to the production of H_2O_2 and other acidic substances. Pure DI water was utilized under the optimal condition for 1 h to be a benchmark in the change of pH and the products from aqueous glycerol. No products were detected by GC-FID, and the pH of the solution remained unchanged, implying that the reactive species from He plasma did not affect the change in water molecules, although they might be excited, being in the form of unstable molecules. Since the system consisted of O and H elements, they could recombine to be stable water molecules after the reaction. Likewise, in glycerol solution, glycerol molecules could be activated by the reactive species producing the DHA, leaving H to incorporate with each other along with electron capturing to become H_2. Additionally, the reaction could further occur to generate other acidic chemicals, such as glyceric acid, as found by NMR analysis in our previous work[35], which exhibits a much higher boiling point (predicted to be 412.0 ± 30.0 °C at atmospheric pressure) than the maximum of GC column temperature to be detected.

The feed glycerol and product at 5 h of reaction time were additionally analyzed by HPLC, as presented in supplementary Fig. S4. For the feed glycerol, there was no peak appearance because the glycerol could not be absorbed by the UV detector[63]. Accordingly, the chromatogram, the glycerol products after the reaction for 5 h consisted of three main produce peaks detected at the peak number of 12.64, 13.43, and 14.56 min corresponding to glyceraldehyde (GLD), glycolic acid (GLYCOA) and DHA, respectively. Additionally, formic acid (FA) was also injected into HPLC and appeared to be absorbed at the time 14.71 min, which was close to the DHA peak. The acid products found in HPLC analysis were related to the peak in the GC chromatogram because their boiling point was close to that of water. The retention time for analysis was up to 30 min, and no other peaks appeared, implying that the main product obtained in the present study was DHA. For the mass balance of the system, feed glycerol of 9.2 g/L was converted into several products at 5 h of reaction time under the most suitable condition. There was a remaining glycerol of 1.60 g/L. The DHA, GLD, and GLYCOA were produced at 2.75, 1.47, and 1.37 g/L, respectively, while 0.42 g/L was others that could be light products, e.g.,

H_2, CO_2. The amount of the detected products was 82.72% of the feed glycerol. In comparison to the study of Walgode et al.[10], the conversion of 1 M aqueous glycerol via catalytic oxidation to DHA and other products using commercial catalysts: Pt/AC and Pt-Bi/AC, the different types and amounts of catalysts affected the conversion and selectivity of products. The mass of all products and remaining glycerol was reported, and the concentration of products achieved 81–87% of feed at the most suitable condition for 1–2 h when Pt5%-Bi1.5%/AC was employed. Several methods for glycerol conversion provided a concentration of approximately 15–97% of the obtained products[13,64,65]. Therefore, the concentration of generated products in this work was within this range.

Plasma reaction mechanism

In the plasma, He gas was partially ionized, creating energetic electrons, He species including helium atoms (He), ions (He^+), radicals ($He^•$), and excited/ metastable helium (He^*). The plasma also produced UV light and heat[66]. When the plasma was generated within the quartz tube immersed in the solution, all these reactive species must have passed through the solution before exiting the reactor. At first, the energetic electrons played a crucial role in this reaction due to their higher mobility compared to ions and radicals, enabling them to move faster[67]. However, to sustain the plasma, metastable helium (He*) atoms and electrons initiate the Penning process by transferring their energy to other atoms, leading to chain ionization and excitation[68]. Nevertheless, the electrons initially played an important role in colliding with other molecules in gas phase; there is rapid energy depletion of them to the surrounding liquid aqueous glycerol. The proposed mechanism of plasma reaction in the present study is shown in Fig. 8. In this plasma system, the water partially evaporated over the solution due to the heat released from the DBD plasma. Therefore, there were two zones where the water molecules could be broken by the plasma reactive species as follows: (1) in the gas phase and (2) at the gas-liquid interface[25]. Water could become an unstable molecule and undergo breakage, forming H•, O•, and OH• radicals when they received sufficient energy[69]. During the process, the water possibly changed to H_2O_2 due to the combination of two OH• radicals when they came to stable molecules[70]. Among the generated radicals, the OH• radicals were essential to initiate the glycerol decomposition[43], and accepted the hydrogen extracted from glycerol, becoming H_2O. Also, H_2 and H_2O_2 could be generated when hydrogen atoms were incorporated with H• and O• radicals. The details of He plasma formation and aqueous glycerol dissociation are described in subplementary Sect. 1, the reaction pathway.

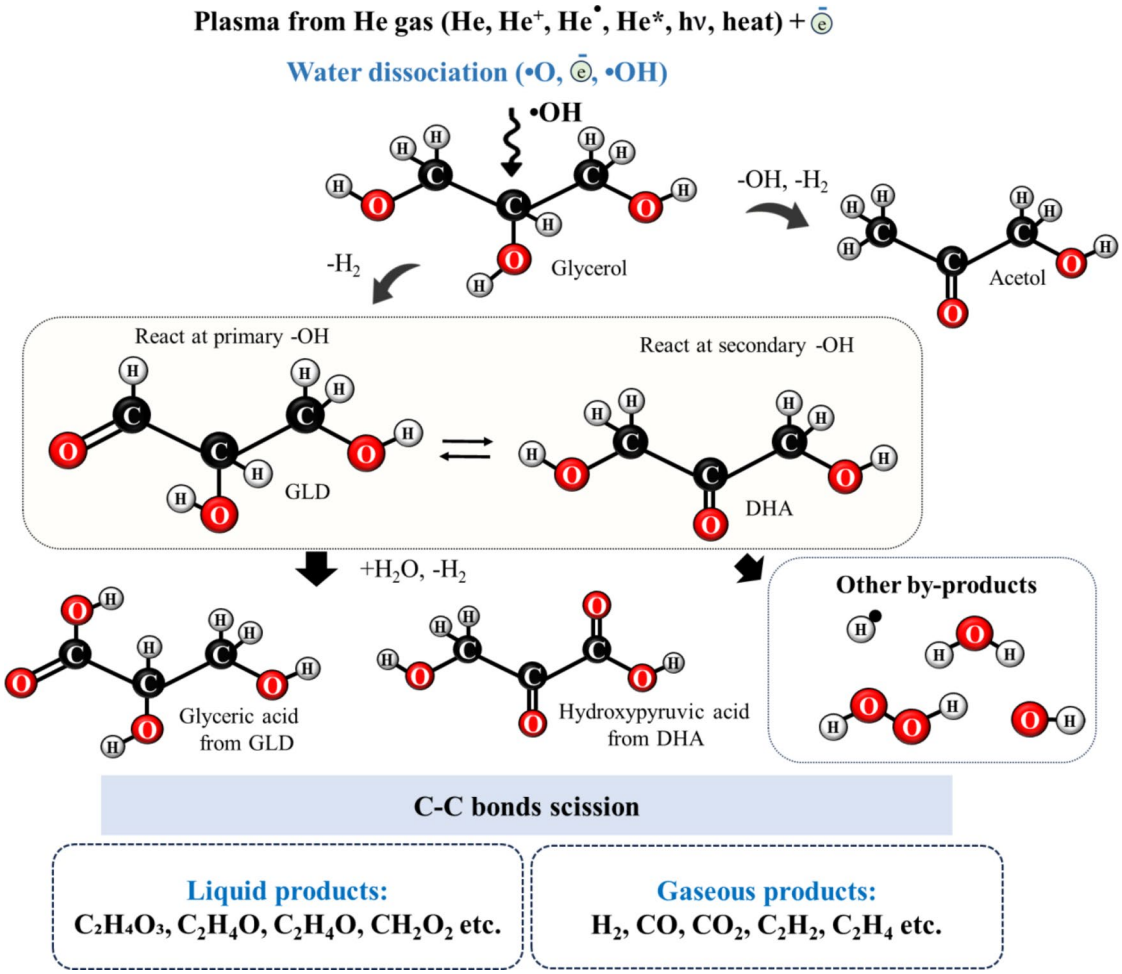

Fig. 8. Proposed plasma mechanism of glycerol dehydrogenation.

Glycerol consists of several types of bonds, including C-C, C–H, C–O, and O–H bonds. Among these, the C-H bond at the secondary carbon position has the lowest energy, making it more susceptible to breaking. Additionally, the hydroxyl group (-OH) bond is relatively weak due to its low activation energy of about 1.93–27.02 kJ/mol[71]. As a result, the reaction primarily occurs through the activation of the secondary C-H and -OH groups, leading to the H atoms leaving — a process commonly called dehydrogenation. Two possible routes can occur during this process. In the first route, the primary -OH group, situated at the two terminal carbons of the glycerol molecule, becomes activated. The hydrogen atom attached to the oxygen is removed, resulting in the formation of an alkoxide. Subsequently, the molecule adjusts to a stable -C=O group, characterized by a high bond dissociation energy (799 kJ/mol), making breaking difficult. The dehydrogenation product of the primary hydroxyl group is glyceraldehyde (GLD), which is formed in this reaction. In the second route, the reaction takes place at the secondary -OH group located at the middle carbon of the glycerol molecule. Following the similar process observed in the primary -OH reaction, the product formed is DHA. The leaving $H^{\bullet}$ radicals can bond with each other and capture electrons, producing hydrogen molecules (H_2). The generated H_2 gas is then carried out of the reactor with the carrier gas. Regarding the dehydrogenation process, DHA is favored over GLD due to the lower energy barrier required for the cleavage of the secondary C-H bond in glycerol, as previously mentioned[72]. The scission of this bond occurs easily, allowing for the formation of the stable C=O group in DHA upon removing another hydrogen atom from the secondary hydroxyl group. After the production of GLD and DHA, the reaction can proceed further by dehydrogenation and incorporating a water molecule to form glyceric acid and hydroxypyruvic acid. This pathway is highly possible to occur since the system is abundant in water. Additionally, during this process, the hydrogen atom can be eliminated simultaneously with the hydroxyl radical, leading to the generation of acetol. The C-C cleavage can take place. However, it is reported that the C-C bond is broken after the dehydrogenation of glycerol occurs significantly[72]. In this study, the cracking process of glycerol formed two acid products, including glycolic acid and formic acid, as presented in the HPLC chromatogram. Furthermore, liquid products like ethanol, ethanediol, and other similar compounds can be formed. These liquid products may undergo further decomposition into gaseous species such as H_2, CO, CO_2, C_2H_2, and others. In the case of gaseous products formed, these gases would leave the reactor with the He carrier gas during the reaction.

Conclusion

The needle-in-tube-type DBD plasma reactor was successfully utilized for glycerol conversion to DHA. The best condition obtained in this investigation was 60 W input power, 5 mm gap distance between the end of the needle and liquid surface, and 0.5 L/min He flow rate. The reaction occurred at ambient temperature and atmospheric pressure in the absence of a catalyst. A glycerol concentration of 0.1 M provided the highest DHA yield of 29.3% at 3 h. At this reaction time, the DHA selectivity and glycerol conversion were 51.6 and 56.9%, respectively. The glycerol continuously reacted with the reactive species in the plasma and reached 82.8% conversion after 5 h of reaction time. This presented novel plasma technique offered superior performance to achieve DHA selectivity and productivity rate over photocatalytic reaction employing a TiO_2 catalyst. Therefore, this DBD plasma technique is a promising way for glycerol valorization. The system is simple and does not require a catalyst, offering advantages in energy saving and environmental consciousness in processes related to a catalyst: preparation, regeneration, removal, and disposal. It has the potential for DHA production from glycerol or crude glycerol dissolved in other solvents such as DMSO, acetonitrile, and so on. However, the process inevitably relied upon the reactive species in the plasma state randomly reacting with glycerol molecules dissolved in water, causing the selectivity to be relatively low. Additionally, the gaseous and liquid by-products of plasma dehydrogenation should be further analyzed to indicate the type of chemicals, which is important for determining the proper separation method of DHA from other products. This DBD plasma technique can be further improved by changing the carrier gas, for different gases offer different energy of reactive species to collide with glycerol, resulting in dehydrogenation.

Data availability

The datasets used and/or analysed during the current study available from the corresponding author on reasonable request.

Received: 31 January 2024; Accepted: 9 December 2024
Published online: 28 December 2024

References

1. Costa, A. A. F. et al. Glycerol and catalysis by Waste/Low-Cost Materials—A review. *Catalysts* **12**, 570 (2022).
2. Dhabhai, R., Koranian, P., Huang, Q., Scheibelhoffer, D. S. B. & Dalai, A. K. Purification of glycerol and its conversion to value-added chemicals: a review. *Sep. Sci. Technol.* **58**, 1383–1402. https://doi.org/10.1080/01496395.2023.2189054 (2023).
3. Abdul Raman, A. A., Tan, H. W. & Buthiyappan, A. Two-step purification of glycerol as a value added by product from the Biodiesel production process. *Front. Chem.* **7**, 774. https://doi.org/10.3389/fchem.2019.00774 (2019).
4. Luo, L. et al. Selective photoelectrocatalytic glycerol oxidation to Dihydroxyacetone via enhanced Middle Hydroxyl Adsorption over a Bi2O3-Incorporated Catalyst. *J. Am. Chem. Soc.* **144**, 7720–7730. https://doi.org/10.1021/jacs.2c00465 (2022).
5. Chilakamarry, C. R., Sakinah, A. M. M., Zularisam, A. W. & Pandey, A. Glycerol waste to value added products and its potential applications. *Syst. Microbiol. Biomanufacturing.* **1**, 378–396. https://doi.org/10.1007/s43393-021-00036-w (2021).
6. Liu, D. et al. Selective photoelectrochemical oxidation of glycerol to high value-added dihydroxyacetone. *Nat. Commun.* **10**, 1779. https://doi.org/10.1038/s41467-019-09788-5 (2019).
7. Bricotte, L., Chougrani, K., Alard, V., Ladmiral, V. & Caillol, S. Dihydroxyacetone: a user guide for a Challenging Bio-based Synthon. *Molecules* **28**, 2724 (2023).

8. Ciriminna, R., Fidalgo, A., Ilharco, L. M. & Pagliaro, M. Dihydroxyacetone: an updated insight into an important Bioproduct. *ChemistryOpen* **7**, 233–236. https://doi.org/10.1002/open.201700201 (2018).
9. An, Z. et al. Insights into the multiple synergies of supports in the selective oxidation of glycerol to Dihydroxyacetone: layered double Hydroxide supported au. *ACS Catal.* **10**, 12437–12453. https://doi.org/10.1021/acscatal.0c02844 (2020).
10. Walgode, M., Coelho, P. D., Faria, L. C. V., Rodrigues, E. & R. P. & Dihydroxyacetone Production: from glycerol Catalytic Oxidation with Commercial catalysts to chromatographic separation. *Ind. Eng. Chem. Res.* **60**, 10551–10565. https://doi.org/10.1021/acs.iecr.1c00275 (2021).
11. Lari, G. M. et al. Environmental and economical perspectives of a glycerol biorefinery. *Energy Environ. Sci.* **11**, 1012–1029. https://doi.org/10.1039/C7EE03116E (2018).
12. Lee, S. et al. Highly selective transformation of glycerol to dihydroxyacetone without using oxidants by a PtSb/C-catalyzed electrooxidation process. *Green Chem.* **18**, 2877–2887. https://doi.org/10.1039/C5GC02865E (2016).
13. Imbault, A. L., Gong, J. & Farnood, R. Photocatalytic production of dihydroxyacetone from glycerol on TiO2 in acetonitrile. *RSC Adv.* **10**, 4956–4968. https://doi.org/10.1039/C9RA09434B (2020).
14. Zhang, Y., Zhang, N., Tang, Z. R. & Xu, Y. J. Identification of Bi2WO6 as a highly selective visible-light photocatalyst toward oxidation of glycerol to dihydroxyacetone in water. *Chem. Sci.* **4**, 1820–1824. https://doi.org/10.1039/C3SC50285F (2013).
15. He, Z. et al. Selective oxidation of glycerol over supported noble metal catalysts. *Catal. Today*. **365**, 162–171. https://doi.org/10.1016/j.cattod.2020.04.019 (2021).
16. Ripoll, M., Jackson, E., Trelles, J. A. & Betancor, L. Dihydroxyacetone production via heterogeneous biotransformations of crude glycerol. *J. Biotechnol.* **340**, 102–109. https://doi.org/10.1016/j.jbiotec.2021.08.011 (2021).
17. Imbault, A. L. & Farnood, R. Selective Oxidation of Crude Glycerol to Dihydroxyacetone in a biphasic photoreactor. *Catalysts* **10**, 360 (2020).
18. Boulos, M. I., Fauchais, P. L. & Pfender, E. in *Handbook of Thermal Plasmas* (eds Maher I. Boulos, Pierre L. Fauchais, & Emil Pfender) 1–53Springer International Publishing, (2016).
19. Liu, L. et al. Extending Catalyst Life in glycerol-to-Acrolein Conversion using non-thermal plasma. *Front. Chem.* **7**, 108 (2019).
20. Harris, J., Phan, A. N. & Zhang, K. Cold plasma catalysis as a novel approach for valorisation of untreated waste glycerol. *Green Chem.* **20**, 2578–2587. https://doi.org/10.1039/C8GC01163J (2018).
21. Liu, L. & Ye, X. P. Nonthermal plasma Induced Fabrication of Solid Acid catalysts for glycerol dehydration to Acrolein. *Catalysts* **11**, 391 (2021).
22. Schwengber, C. A. et al. Overview of glycerol reforming for hydrogen production. *Renew. Sustain. Energy Rev.* **58**, 259–266 (2016).
23. Sakakura, T. et al. Excitation of H2O at the plasma/water interface by UV irradiation for the elevation of ammonia production. *Green Chem.* **20**, 627–633. https://doi.org/10.1039/C7GC03007J (2018).
24. Haruyama, T. et al. Non-catalyzed one-step synthesis of ammonia from atmospheric air and water. *Green Chem.* **18**, 4536–4541. https://doi.org/10.1039/C6GC01560C (2016).
25. Harris, J., Zhang, K. & Phan, A. N. Cold plasma assisted deoxygenation of liquid phase glycerol at atmospheric pressure. *Chem. Eng. J.* **393**, 124698. https://doi.org/10.1016/j.cej.2020.124698 (2020).
26. Tamošiūnas, A. et al. Energy recovery from waste glycerol by utilizing thermal water vapor plasma. *Environ. Sci. Pollut. Res.* **24**, 10030–10040. https://doi.org/10.1007/s11356-016-8097-8 (2017).
27. Tamošiūnas, A., Gimžauskaitė, D., Aikas, M., Uscila, R. & Zakarauskas, K. Waste glycerol gasification to syngas in pure DC water vapor arc plasma. *Int. J. Hydrog. Energy*. **47**, 12219–12230. https://doi.org/10.1016/j.ijhydene.2021.06.203 (2022).
28. Uytdenhouwen, Y. et al. A packed-bed DBD micro plasma reactor for CO2 dissociation: does size matter? *Chem. Eng. J.* **348**, 557–568. https://doi.org/10.1016/j.cej.2018.04.210 (2018).
29. Wongjaikham, W. et al. Highly effective microwave plasma application for catalyst-free and low temperature hydrogenation of biodiesel. *Fuel* **305**, 121524. https://doi.org/10.1016/j.fuel.2021.121524 (2021).
30. Hao, H. et al. Non-thermal plasma enhanced heavy oil upgrading. *Fuel* **149**, 162–173. https://doi.org/10.1016/j.fuel.2014.08.043 (2015).
31. Puprasit, K., Wongsawaeng, D., Ngaosuwan, K., Kiatkittipong, W. & Assabumrungrat, S. Improved hydrogenation process for margarine production with no trans fatty acid formation by non-thermal plasma with needle-in-tube configuration. *J. Food Eng.* **334**, 111167. https://doi.org/10.1016/j.jfoodeng.2022.111167 (2022).
32. Yepez, X. V. & Keener, K. M. High-voltage Atmospheric Cold plasma (HVACP) hydrogenation of soybean oil without trans-fatty acids. *Innovative Food Sci. Emerg. Technol.* **38**, 169–174. https://doi.org/10.1016/j.ifset.2016.09.001 (2016).
33. Kamjam, M. et al. Upgrading palm biodiesel properties via catalyst-free partial hydrogenation using needle-plate dielectric barrier discharge plasma torch. *Int. J. Energy Res.* **46**, 11756–11777. https://doi.org/10.1002/er.7944 (2022).
34. Kongprawes, G. et al. Improvement of oxidation stability of fatty acid methyl esters derived from soybean oil via partial hydrogenation using dielectric barrier discharge plasma. *Int. J. Energy Res.* **45**, 4519–4533. https://doi.org/10.1002/er.6121 (2021).
35. Kongprawes, G. et al. Dielectric barrier discharge plasma for catalytic-free palm oil hydrogenation using glycerol as hydrogen donor for further production of hydrogenated fatty acid methyl ester (H-FAME). *J. Clean. Prod.* **401**, 136724. https://doi.org/10.1016/j.jclepro.2023.136724 (2023).
36. Parodi, A., Diguilio, E., Renzini, S. & Magario, I. An alternative approach for quantification of glyceraldehyde and dihydroxyacetone as trimethylsilyl derivatives by GC-FID. *Carbohydr. Res.* **487**, 107885. https://doi.org/10.1016/j.carres.2019.107885 (2020).
37. Wu, J., Li, M. H., Lin, J. P. & Wei, D. Z. Determination of dihydroxyacetone and glycerol in fermentation process by GC after n-methylimidazole catalyzed acetylation. *J. Chromatogr. Sci.* **49**, 375–378. https://doi.org/10.1093/chromsci/49.5.375 (2011).
38. Egoburo, D. E., Diaz Peña, R., Kolender, A. & Pettinari, M. J. Optimization and validation of a GC–FID method for quantitative determination of 1,3-Propanediol in Bacterial Culture Aqueous supernatants containing glycerol. *Chromatographia* **80**, 1121–1127. https://doi.org/10.1007/s10337-017-3310-6 (2017).
39. Lili, W., Jie, Q., Zhongce, H., Yuguo, Z. & Wei, H. Determination of dihydroxyacetone and glycerol in fermentation broth by pyrolytic methylation/gas chromatography. *Anal. Chim. Acta*. **557**, 262–266. https://doi.org/10.1016/j.aca.2005.10.030 (2006).
40. Liebminger, S., Siebenhofer, M. & Guebitz, G. Oxidation of glycerol by 2,2,6,6-tetramethylpiperidine-N-oxyl (TEMPO) in the presence of laccase. *Bioresour. Technol.* **100**, 4541–4545. https://doi.org/10.1016/j.biortech.2009.04.051 (2009).
41. Nascimento, F., Kostov, K. G., Machida, M. & Flacker, A. Properties of DBD plasma jets using Powered Electrode with and without contact with the plasma. *IEEE Trans. Plasma Sci.* **49**, 1293–1301. https://doi.org/10.1109/TPS.2021.3067159 (2021).
42. Du, Y., Nayak, G., Oinuma, G., Peng, Z. & Bruggeman, P. J. Effect of water vapor on plasma morphology, OH and H2O2 production in he and Ar atmospheric pressure dielectric barrier discharges. *J. Phys. D.* **50**, 145201. https://doi.org/10.1088/1361-6463/aa5e7d (2017).
43. Bang, S., Snoeckx, R. & Cha, M. S. Valorization of Glycerol through Plasma-Induced Transformation into Formic Acid. *ChemSusChem* 17, e202300925, doi: (2024). https://doi.org/10.1002/cssc.202300925
44. Zigon, J., Petric, M. & Dahle, S. Dielectric barrier discharge (DBD) plasma pretreatment of lignocellulosic materials in air at atmospheric pressure for their improved wettability: a literature review. *Holzforschung* **72**, 979–991 (2018).
45. Hosseinpour, M. & Zendehnam, A. Study of an argon dielectric barrier discharge reactor with atmospheric pressure for material treatment. *J. Theoretical Appl. Phys.* **12**, 271–291. https://doi.org/10.1007/s40094-018-0316-x (2018).
46. Hoft, H., Becker, M. M. & Kettlitz, M. Impact of gas flow rate on breakdown of filamentary dielectric barrier discharges. *Phys. Plasmas*. **23**, 033504 (2016).

47. Qiang, S. et al. A novel experimental method of investigating anode-arc-root behaviors in a DC non-transferred arc plasma torch. *Plasma Sources Sci. Technol.* **29**, 025008. https://doi.org/10.1088/1361-6595/ab652e (2020).
48. Saini, R. K., Kuchlyan, J. & Sarkar, N. Effect of viscosity on photoinduced electron transfer reaction: an observation of the Marcus inverted region in homogeneous solvents. *Chem. Phys. Lett.* **660**, 81–86. https://doi.org/10.1016/j.cplett.2016.08.007 (2016).
49. Schmidt, W. F., Hilt, O., Illenberger, E. & Khrapak, A. G. The mobility of positive and negative ions in liquid xenon. *Radiat. Phys. Chem.* **74**, 152–159. https://doi.org/10.1016/j.radphyschem.2005.04.008 (2005).
50. Mendoza, A. et al. Selective production of dihydroxyacetone and glyceraldehyde by photo-assisted oxidation of glycerol. *Catal. Today*. **358**, 149–154. https://doi.org/10.1016/j.cattod.2019.09.035 (2020).
51. Ye, Z. et al. Feasibility of destruction of gaseous benzene with dielectric barrier discharge. *J. Hazard. Mater.* **156**, 356–364. https://doi.org/10.1016/j.jhazmat.2007.12.048 (2008).
52. Okubo, M. Recent development of technology in scale-up of plasma reactors for Environmental and Energy Applications. *Plasma Chem. Plasma Process.* **42**, 3–33. https://doi.org/10.1007/s11090-021-10201-7 (2022).
53. Xu, M. et al. Design and characterization of an Upscaled Dielectric Barrier Discharge-based ten-layer plasma source for High-Flow-Rate Gas treatment. *Appl. Sci.* **14** (2024).
54. Durek, J. et al. Pilot-scale generation of plasma processed air and its influence on microbial count, microbial diversity, and selected quality parameters of dried herbs. *Innovative Food Sci. Emerg. Technol.* **75**, 102890. https://doi.org/10.1016/j.ifset.2021.102890 (2022).
55. Misra, N. N., Sreelakshmi, V. P., Naladala, T., Alzahrani, K. J. & Negi, P. S. Design and construction of a continuous industrial scale cold plasma equipment for fresh produce industry. *Innovative Food Sci. Emerg. Technol.* **97**, 103840. https://doi.org/10.1016/j.ifset.2024.103840 (2024).
56. Zhao, Y. et al. Decomposition of VOCs by a novel catalytic DBD plasma reactor: a pilot study. *ChemistrySelect* **7**, e202201614. https://doi.org/10.1002/slct.202201614 (2022).
57. Saoud, W. A. et al. Pilot scale investigation of DBD-Plasma photocatalysis for industrial application in livestock building air: elimination of chemical pollutants and odors. *Chem. Eng. J.* **468**, 143710. https://doi.org/10.1016/j.cej.2023.143710 (2023).
58. Chen, M. et al. Development of an industrial applicable dielectric barrier discharge (DBD) plasma treatment for improving bondability of poplar veneer. **70**, 683–690, doi:doi: (2016). https://doi.org/10.1515/hf-2015-0122
59. Adeniyi, A. G. & Ighalo, J. O. A review of steam reforming of glycerol. *Chem. Pap.* **73**, 2619–2635. https://doi.org/10.1007/s11696-019-00840-8 (2019).
60. Sun, Y., Lee, S. & Lin, L. Comparison of Color Development Kinetics of tanning reactions of Dihydroxyacetone with Free and protected basic amino acids. *ACS Omega*. **7**, 45510–45517 (2022).
61. Salehpour, S. & Dubé, M. A. Reaction monitoring of glycerol step-growth polymerization using ATR-FTIR spectroscopy. *Macromol. React. Eng.* **6**, 85–92. https://doi.org/10.1002/mren.201100071 (2012).
62. Zhuang, J., Li, M., Pu, Y., Ragauskas, A. J. & Yoo, C. G. Observation of potential contaminants in processed Biomass using Fourier transform Infrared Spectroscopy. *Appl. Sci.* **10**, 4345 (2020).
63. Beltrán-Prieto, J. C., Pecha, J., Kašpárková, V., Kolomazník, K. & DEVELOPMENT OF AN HPLC METHOD FOR THE DETERMINATION OF GLYCEROL OXIDATION PRODUCTS. *J. Liq. Chromatogr. Relat. Technol.* **36**, 2758–2773, doi:https://doi.org/10.1080/10826076.2012.725695 (2013).
64. Wang, Y., Liu, W., Zhao, J., Wang, Z. & Zhao, N. Oxidation of glycerol to dihydroxyacetone over highly stable au catalysts supported on mineral-derived CuO-ZnO mixed oxide. *Appl. Catal. A*. **671**, 119578. https://doi.org/10.1016/j.apcata.2024.119578 (2024).
65. Nunotani, N., Takashima, M., Choi, P. G., Choi, Y. B. & Imanaka, N. Selective oxidation of glycerol to dihydroxyacetone using CeO2-ZrO2-Bi2O3-SnO2-supported platinum catalysts. *J. Asian. Ceam. Soc.* **8**, 470–475. https://doi.org/10.1080/21870764.2020.1753915 (2020).
66. Nguyen, D. V., Ho, P. Q., Pham, T. V., Nguyen, T. V. & Kim, L. Treatment of surface water using cold plasma for domestic water supply. *Environ. Eng. Res.* **24**, 412–417. https://doi.org/10.4491/eer.2018.215 (2018).
67. Vadikkeettil, Y. et al. Plasma assisted decomposition and reforming of greenhouse gases: a review of current status and emerging trends. *Renew. Sustain. Energy Rev.* **161**, 112343. https://doi.org/10.1016/j.rser.2022.112343 (2022).
68. Mattox, D. M. in *In Handbook of Physical Vapor Deposition (PVD) Processing (Second Edition)*. 157–193 (eds Mattox, D. M.) (William Andrew Publishing, 2010).
69. Cheng, J. et al. Mechanism and reactive species in a Fountain-Strip DBD plasma for degrading perfluorooctanoic acid (PFOA). *Water* **14**, 3384 (2022).
70. Cameli, F., Dimitrakellis, P., Chen, T. Y. & Vlachos, D. G. Modular plasma microreactor for intensified hydrogen peroxide production. *ACS Sustain. Chem. Eng.* **10**, 1829–1838. https://doi.org/10.1021/acssuschemeng.1c06973 (2022).
71. Wan, W. et al. Controlling reaction pathways of selective C–O bond cleavage of glycerol. *Nat. Commun.* **9**, 4612. https://doi.org/10.1038/s41467-018-07047-7 (2018).
72. Liu, B. & Greeley, J. Decomposition pathways of glycerol via C–H, O–H, and C–C bond scission on pt(111): a density functional theory study. *J. Phys. Chem. C.* **115**, 19702–19709. https://doi.org/10.1021/jp202923w (2011).

Acknowledgements

This project is funded by the Second Century Fund (C2F) of Chulalongkorn University, This Quick Win research project is supported by Ratchadapiseksompotch Fund Chulalongkorn University, D. Wongsawaeng, K. Ngaosuwan, W. Kiatkittipong, and S. Assabumrungrat also would like to acknowledge the supports from the NSRF via the Program Management Unit from Human Resources & Institutional Development, Research and Innovation (Grant number B05F640085) and The Office of the Permanent Secretary of the Ministry of Higher Education, Science, Research and Innovation (Reinventing University Grant).

Author contributions

G.K.: Investigation, Writing- original draft, Funding acquisition.D.W. : Conceptualization, Methodology, Resources, Writing- original draft, Writing- review & editing, Funding acquisition.P.H. : Supervision.K.N. : Writing- review & editing. W.K. : Writing- review & editing. S.A.: Supervision, Writing- review & editing.

Declarations

Competing interests

The authors declare no competing interests.

Additional information

Supplementary Information The online version contains supplementary material available at https://doi.org/1

0.1038/s41598-024-82691-2.

Correspondence and requests for materials should be addressed to D.W.